PHYSICAL REVIEW B VOLUME 51, NUMBER 4 15 JANUARY 1995-II

Self-annihilation of surface precipitates on compound films by alternate impinging of molecular beams

Masanori Yata and Keikichi Nakamura
National Research Institute for Metals, 1-2-1 Sengen, Tsukuba, Ibaraki 305, Japan

Keiichi Ogawa
Yokohama City University, 22-2 Seto, Kanazawa-ku, Yokohama, Kanagawa 236, Japan

(Received 4 April 1994; revised manuscript received 22 August 1994)

Surface precipitates, resulting from the compositional deviation in the growth of compound films, can be annihilated by impingement of elements that are necessary for the precipitates to assimilate into the underlying stoichiometric compound, and such phenomena are found to occur at a substrate temperature above the melting point of the surface precipitates. We report on the annihilation of Pd-rich Te precipitates on PdTe(001) films through the impingement of a Te_2 molecular beam. The Pd-rich Te precipitates, which are liquid above 620 K, are formed by the impingement of excess Pd atoms on the Pd-terminated PdTe(001)-$(\sqrt{3}\times\sqrt{3})R30°$ surface. When the Te_2 molecular beam impinges onto the surface at above 620 K, Te_2 molecules are captured on the Pd-terminated $(\sqrt{3}\times\sqrt{3})R30°$ surface and the liquid precipitates with the sticking probability of unity. The excess Pd liberated from the liquid precipitates moves across the surface to form a planar Pd-terminated PdTe(001) surface until the precipitate assimilates into the underlying stoichiometric compound. After the assimilation, the Te-terminated PdTe(001)-(1×1) surface appears. Thus the alternating impingement of Pd and Te_2 beams onto the PdTe substrate repeats the process of generation and annihilation of the liquid precipitates; consequently precipitate-free epitaxial growth occurs. A possible growth mechanism is proposed.

I. INTRODUCTION

The precipitation of impure phases resulting from compositional deviation must be removed to grow high-quality compound films such as semiconductor or superconductor films. In molecular beam epitaxy (MBE), for instance, fluctuation of growth conditions such as flux of molecular beams or substrate temperature causes surface precipitates.[1–4] Once precipitates are generated, it is often difficult to annihilate them by changing the growth conditions.

One of the most simple cases on the annihilation of surface precipitates is the growth of the GaAs compound in migration-enhanced epitaxy (MEE) (Refs. 5 and 6) and droplet epitaxy (DE).[7,8] GaAs is only a compound phase in the Ga-As system; excess Ga on GaAs forms liquid precipitates of Ga (Ga droplets) at the substrate temperature above room temperature (RT), and then the Ga droplets crystallize to form GaAs upon the impingement of the As molecular beam. As Ga droplets wet the GaAs substrate surface under the impingement of As molecules, the Ga droplets crystallize two-dimensionally to form GaAs with a flat surface (i.e., MEE). Ga droplets on sulfur-terminated GaAs, however, do not wet the substrate surface. Therefore, the droplets form three-dimensional microcrystals of GaAs (DE).

Ga precipitation on GaAs, however, is a unique phenomenon in the III-V compounds for near stoichiometric growth.[4] InSb precipitation on InSb seems to be more appropriate to the case. According to the three-dimensional (composition, temperature, vapor pressure) phase diagram for InSb reported by Tsao,[9] the pressure and temperature region within which InSb MBE growth is thermodynamically favored over condensation of other phases is very narrow. Consequently, an InSb compound, even as it grows, will itself tend to decompose into In-rich liquid plus Sb-rich vapor. By this phase diagram, Sb vapor pressure (flux) and the substrate temperature necessary for annihilation of the In-rich precipitates on the underlying InSb film can be predicted. Thus the three-dimensional phase diagram is a useful chart to determine the growth condition for annihilation of the surface precipitates, although it does not involve a timescale.

Recently we found that the growth of PdTe intermetallic compound film is a case in which self-annihilation of a surface precipitate occurs. PdTe is one of many transition-metal–chalcogenide compounds. The transition-metal–chalcogenide compounds seem to be favorable for MBE growth because the vapor pressure of the transition metal and that of cholcogen are very different. Some difficulties for the MBE growth, however, may be to obtain the single phase required and to control the stoichiometry by controlling each flux of the molecular beam and the substrate temperature. In a previous paper, we reported on the growth of three kinds of Pd-Te intermetallic compounds by MBE: PdTe(001), $Pd_9Te_4(010)$, and $PdTe_2(001)$, and constructed the MBE phase diagram depending on the Pd flux, the Te_2 flux, and the substrate temperature,[10] which can be partially comparable to the three-dimensional phase diagram. In this diagram, the MBE region of the PdTe single phase is very narrow, and the excess Pd flux condition tends to form Pd-rich Te precipitates such as Pd_9Te_4 on the underlying PdTe film. For the annihilation of the Pd-rich Te precipitates, the impingement of Te_2 flux with appropriate intensity and exposure time at the substrate temperature above the melting point of the precipitates is necessary. We have formed Pd-rich precipitates by the impingement of excess Pd atoms on the PdTe(001) films, and have examined the annihilation process of the precipitates through the impingement of Te_2 molecules.

PdTe as well as $PdTe_2$ are of layered structure: NiAs-type PdTe can be regarded as an alternate stacking of Pd and Te close-packed planes along the c axis, and CdI_2-type $PdTe_2$ as a successive stacking of a closed-packed plane unit, Pd/Te/Te, along the c axis. They are superconductors and their critical temperatures strongly depend on their stoichiometry, although neither pure Pd nor pure Te is a superconductor.[11] Thus the control of stoichiometry of these compounds as well as the synthesis of artificially stacked Pd-Te superlattices by MBE are of interest for the synthesis of superconducting layered compounds.

II. EXPERIMENTAL PROCEDURES

The experiments were carried out in an ultrahigh-vacuum (UHV) system (Vacuum Generators V-80 MBE) equipped with reflection high-energy electron diffraction (RHEED). The experimental apparatus was presented in detail elsewhere.[10] The molecular beams of Pd and Te_2 were generated with an electron-beam evaporator and a pyrolitic boron nitride effusion cell, respectively. The Pd flux $J(\mathrm{Pd})$ was kept constant in the range between 6.8×10^{13} and 2.7×10^{14} atoms/cm^2 s, with fluctuations less than 6.8×10^{12} atoms/cm^2 s. The Te_2 flux $J(\mathrm{Te}_2)$ was kept constant in the range between 1.0×10^{13} and 1.7×10^{15} molecules/cm^2 s, with fluctuations less than 3.0×10^{12} molecules/cm^2 s. The PdTe(001) films were grown on 2H-MoS_2(0001) by molecular-beam epitaxy,[10] and the resultant composite crystals were used as substrates. The substrate temperatures were monitored by Pt-(Pt-13%Rh) thermocouples attached behind the substrate holder. The temperatures were calibrated by measuring temperatures of the substrate surface using thermocouples directly attached to the substrate surface, and were additionally calibrated by observing the melting point of 1-μm-thick Sn film deposited on a 2H-MoS_2(0001) substrate by RHEED. The substrate temperature was kept constant at a temperature between 620 and 700 K.

The surface structures of PdTe(001) films were observed *in situ* by means of RHEED operated at 22 kV. The RHEED patterns during the impingement of Pd and/or Te_2 beams were recorded by video-camera recorder (SONY EDC-50), and/or the intensity of a selected part of the RHEED patterns was monitored through a lens system equipped with a photodiode. The surface morphologies and surface compositions were characterized by high-resolution scanning electron microscopy (HRSEM) and by x-ray microanalysis (XMA), respectively. The structure and crystallinity of the films grown were analyzed afterwards by x-ray diffraction (XRD) as well.

III. RESULTS AND DISCUSSION

A. PdTe(001) surfaces

Two kinds of surface structures, namely (1×1) and reconstructed $(\sqrt{3}\times\sqrt{3})R30°$ surfaces, have been observed in the MBE-grown PdTe(001) films. The RHEED observation shows that the impingement of a Te_2 beam onto the (1×1) surface does not change the pattern, while the impingement of a Pd beam transforms the (1×1) pattern to $(\sqrt{3}\times\sqrt{3})R30°$. The $(\sqrt{3}\times\sqrt{3})R30°$ pattern changes to (1×1) by the impingement of a Te_2 beam, while the pattern remains the same by the impingement of a Pd beam. Since PdTe can be regarded as an alternate stacking of Pd and Te close-packed planes along the [001] direction, it appears that the PdTe(001)-(1×1) surface is a Te-terminated or Te-rich one, and that the PdTe(001)-$(\sqrt{3}\times\sqrt{3})R30°$ surface is a Pd-terminated or Pd-rich one.

B. Self-annihilation of surface precipitates

Figure 1 shows the time dependence of the RHEED intensity for the specular and $\frac{1}{3}\frac{1}{3}$ fractional order reflection as the Pd beam is impinged onto the (1×1) surface. The incident electron beam was along the [100] azimuth, and the incident angle was $1.73°\pm0.02°$. On impinging the Pd beam, the specular intensity was reduced and eventually leveled off at lower intensity. With the above change in the specular intensity, the RHEED pattern itself changed from (1×1) to $(\sqrt{3}\times\sqrt{3})R30°$ and the intensity of the $\frac{1}{3}\frac{1}{3}$ fractional order reflection of $(\sqrt{3}\times\sqrt{3})R30°$ increased to a certain level as shown in Fig. 1. Each intensity became constant after a 6.0-s exposure to the Pd beam. The Pd flux $J(\mathrm{Pd})$ was 1.7×10^{14} atoms/cm^2 s. Assuming that the sticking probability of Pd is unity, the saturation coverage of Pd which is sufficient to form the $(\sqrt{3}\times\sqrt{3})R30°$ surface is estimated to be 1.75 monolayers (ML) [i.e., Pd-terminated $(\sqrt{3}\times\sqrt{3})R30°$]. Further impingement of the Pd beam did not change the pattern. Since the sticking probability of Pd was constant and independent of the coverage, as mentioned below, excess Pd atoms after the saturation coverage were condensed on the $(\sqrt{3}\times\sqrt{3})R30°$ surface [i.e., Pd-rich $(\sqrt{3}\times\sqrt{3})R30°$]. The RHEED pattern, however, did not show any crystal structures other than $(\sqrt{3}\times\sqrt{3})R30°$, indicating that the excess Pd atoms formed liquid (or amorphous) precipitates of a Pd-Te mixture at the present substrate temperatures employed, i.e., temperatures between 620 and 700 K. Examinations of the samples with HRSEM and XMA confirmed the presence of Pd-rich precipitates on the underlying PdTe surface, as shown in Fig. 2(a). The results of XRD showed that the precipitates have Pd_9Te_4(010) structure at room temperature. Thus we conclude that the excess Pd atoms on the $(\sqrt{3}\times\sqrt{3})R30°$ surface form the liquid precipitates of the composition lying between PdTe and Pd_9Te_4 at a substrate temperature above 620 K. The reaction is described by the following process:

$$\text{PdTe-solid}+\text{Pd}\rightarrow(\text{Pd-rich Te})\ \text{liquid}\ , \tag{1}$$

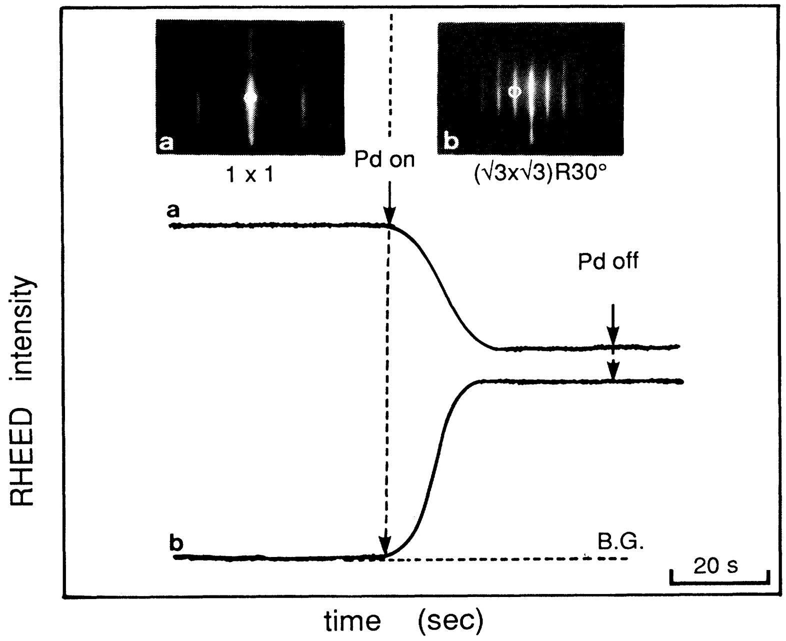

FIG. 1. Changes of the RHEED intensity and the corresponding RHEED patterns during the impingement of the Pd beam on PdTe(001). Curve a: specular intensity. Curve b: intensity of $\frac{1}{3}\frac{1}{3}$ fractional order reflection. Pattern (a): surface structure of Te-terminated PdTe(001)-(1×1). The position at which the specular intensity was measured is shown by the white open circle. Pattern (b): surface reconstructed structure of the Pd-terminated or Pd-rich PdTe(001)-$(\sqrt{3}\times\sqrt{3})R30°$. The position at which the intensity of $\frac{1}{3}\frac{1}{3}$ fractional order reflection was measured is shown by the white open circle.

and the liquid precipitates crystallize to form $Pd_9Te_4(010)$ precipitates when the surface is cooled to room temperature.

According to the atmospheric pressure phase diagram of Pd-Te, the liquid phase of the Pd-Te mixture coexists with the PdTe phase in the composition range between Pd-37 at. % Te to Pd-50.5 at. % Te above the temperature of 780 K. The growth temperature 620 K for the present liquid phase of Pd-rich Te mixture, however, is lower by 160 K than the solidification temperature in the atmospheric pressure phase diagram. This depression of the solidification temperature may be explained by considering the phase equilibrium between solid, liquid, and vapor phases far *below atomospheric pressure.* Unfor-

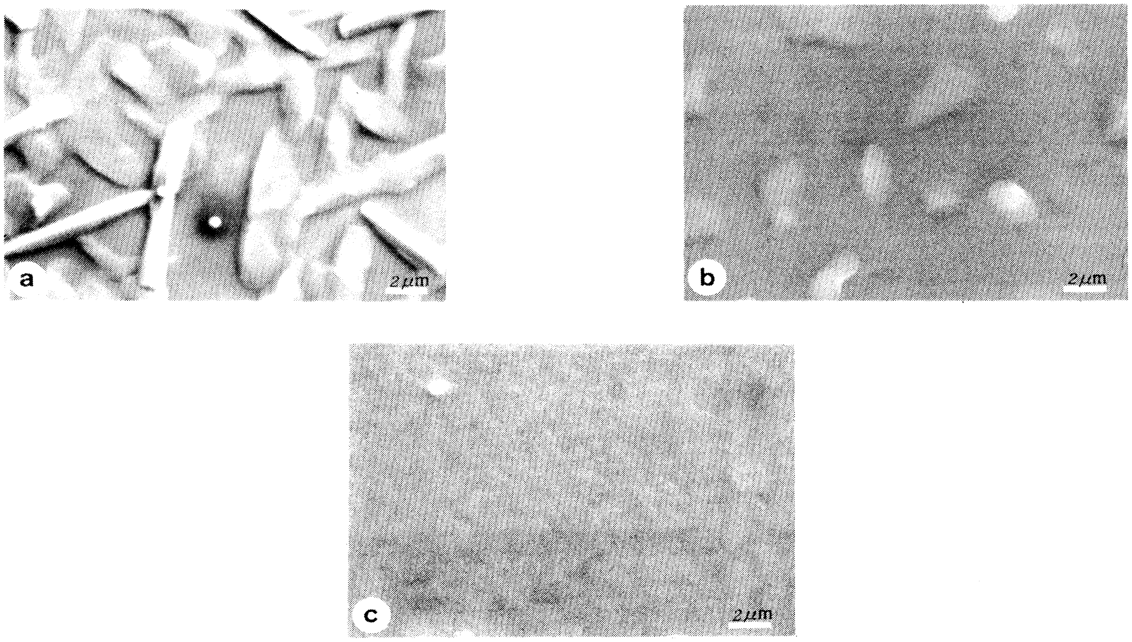

FIG. 2. Surface morphology of the sample. (a) Pd-rich PdTe(001)-$(\sqrt{3}\times\sqrt{3})R30°$ surface. The precipitates of Pd_9Te_4 (010) existed on the underlying PdTe surface. (b) Pd-rich PdTe(001)-$(\sqrt{3}\times\sqrt{3})R30°$ surface after the impingement of a Te_2 beam. The exposure time of the Te_2 beam was shorter than τ_{Te}. (c) Te-terminated PdTe(001)-(1×1) surface after the annihilation of the $Pd_9Te_4(010)$ precipitates.

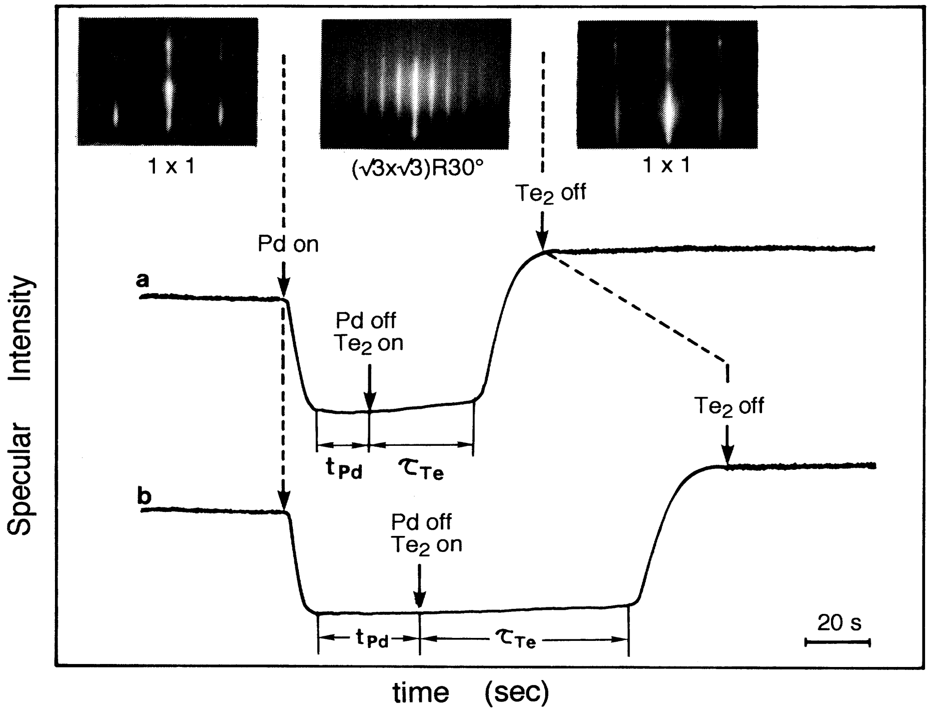

FIG. 3. Changes of the RHEED specular intensity and the corresponding RHEED patterns during alternate impingement of Pd and Te_2 beams. Curve *a*: $t_{Pd}=15$ s; curve *b*: $t_{Pd}=30$ s. $J(Pd)=1.7\times10^{14}$ atoms/cm^2 s. $J(Te_2)=4.0\times10^{13}$ molecules/cm^2 s.

tunately, no such phase diagram is known for the Pd-Te system. We point out, however, that a large comparable depression in the solidification temperature has been predicted from the calculated three-dimensional phase diagram of the III-V compound, i.e., InSb.[9]

As the Te_2 beam impinged onto the Pd-rich PdTe(001)-$(\sqrt{3}\times\sqrt{3})R30°$ surface on which the liquid precipitates existed, the RHEED specular intensity rapidly increased to a certain level only after a certain induction period and the $(\sqrt{3}\times\sqrt{3})R30°$ pattern changed to Te-terminated (1×1), as shown in Fig. 3. The XRD study showed that the Te-terminated $-(1\times1)$ sample consisted of a PdTe(001) single phase, and the HRSEM image showed that the surface was fairly flat without surface precipitates, as shown in Fig. 2(c). Figure 3 shows that the induction period during the impingement of the Te_2 beam (τ_{Te}) depends on the exposure time of the Pd beam after the completion of saturation coverage (t_{Pd}); when t_{Pd} is doubled, τ_{Te} becomes twice as long. Figure 4 clearly shows the following empirical relationship:

$$J(Pd)t_{Pd}=2J(Te_2)\tau_{Te}\ , \tag{2}$$

where $J(Pd)$ and $J(Te_2)$ are fluxes of Pd and Te_2 beams, respectively. Equation (2) shows that an amount of the impinging Pd atoms during t_{Pd} is equal to that of the subsequently impinging Te atoms during τ_{Te}. Thus the liquid precipitates of Pd-rich Te mixture can be transformed completely into PdTe(001):

$$\text{(Pd-rich Te) liquid}+\text{Te}\rightarrow\text{PdTe(001)}\ . \tag{3}$$

Equation (2) suggests that the sticking probability of Pd on PdTe(001) is equal to that of Te_2 on PdTe(001), and that their sticking probabilities are constant as long as the $(\sqrt{3}\times\sqrt{3})R30°$ surface structure is preserved. As the vapor pressure of Pd(gas) over solid Pd at the temperature in the range 620 K is negligible, the sticking probability of Pd is safely assumed as unity; therefore the sticking probability of Te_2 on the Pd-rich $(\sqrt{3}\times\sqrt{3})R30°$ surface should be unity as well. The unity of the Te_2 sticking probability is found to hold for the impinging Te_2 flux ranging from 10^{13} to 10^{15} molecules/cm^2 s. The vapor pressure of Te_2 over solid Te at the temperature in the

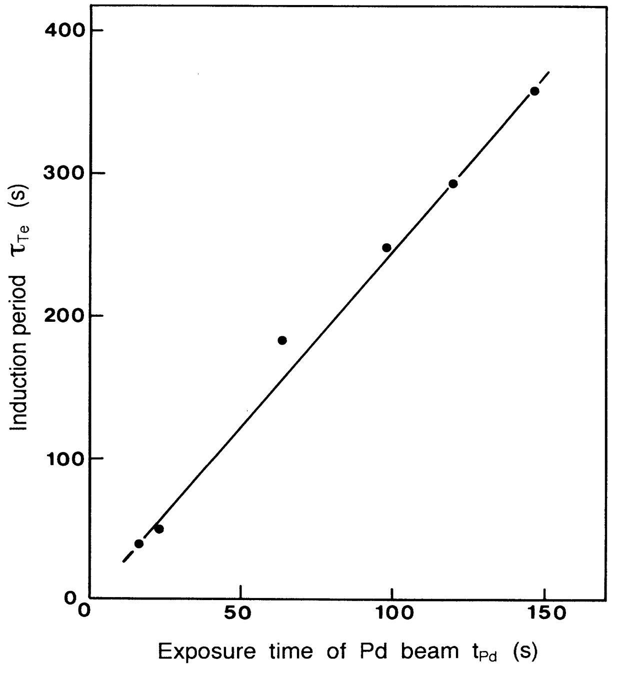

FIG. 4. Induction period (τ_{Te}) depending on exposure time of Pd beam (t_{Pd}). $J(Pd)=1.7\times10^{14}$ atoms/cm^2 s. $J(Te_2)=3.3\times10^{13}$ molecules/cm^2 s.

range 620 K is about 10^{-3} Torr, which corresponds to much higher flux (10^{16} molecules/cm^2 s) as compared with the impinging Te_2 flux employed in this experiment. It is likely, therefore, that the Te_2 molecules impinging onto the Pd-rich $(\sqrt{3}\times\sqrt{3})R30°$ surface do not form a condensed Te phase but are directly trapped on the Pd-terminated $(\sqrt{3}\times\sqrt{3})R30°$ surface region and on the (Pd-rich Te) liquid precipitates. Although any self-limiting adsorption process such as observed in the atomic layer epitaxy (ALE)[12,13] is not applicable to the PdTe compound, the definite atomic layer-by-layer growth of PdTe(001) can be performed through the alternating impingement of Pd and Te_2 beams by monitoring the RHEED intensity and patterns. Even if Pd-rich Te precipitates were formed by the excess Pd impingement, subsequent impingement of the Te_2 beam could annihilate the precipitates to form a stoichiometric PdTe film.

C. Growth mechanism

Based on the experimental results presented in Sec. III B, we propose a mechanism for the self-annihilation of surface precipitates in the epitaxial growth of PdTe (Fig. 5). The impingement of a Pd beam onto the PdTe(001)-Te-terminated(1×1) surface [Fig. 5(a)] changes the surface structure to Pd-terminated $(\sqrt{3}\times\sqrt{3})R30°$ [Fig. 5(b)], and further impingement of the Pd beam produces the liquid precipitates of the Pd-rich Te mixture on the surface when the substrate temperature is above 620 K [Fig. 5(c)]. In cooling the substrate to room temperature, the precipitates crystallize to form $Pd_9Te_4(010)$ [Fig. 5(d)]. When the temperature is above 620 K, the Te_2 molecules impinging directly onto the liquid precipitates are once tapped there, as shown in Fig. 5(e). The other Te_2 molecules, adsorbed on the surfaces of the $(\sqrt{3}\times\sqrt{3})R30°$ region are also trapped by the precipitates after the surface migration. The trapped Te_2 are eventually dissolved in the liquid precipitates altogether. With an increase in the Te concentration of the precipitates, the liquid precipitates crystallize to form PdTe. The crystallized PdTe inherits the orientation of the PdTe(001) substrate. The liquid precipitates play another role in supplying Pd atoms to the $(\sqrt{3}\times\sqrt{3})R30°$ surface region and keeping the surface structure Pd terminated $(\sqrt{3}\times\sqrt{3})R30°$ during the Te_2 beam impingement onto the PdTe surface. It is the excess Pd which moves across the surface, resulting in a planar surface as the film tries to minimize the surface free energy for a stoichiometric PdTe film. Consequently the $(\sqrt{3}\times\sqrt{3})R30°$ surface structure does not change until the precipitates vanish. The induction period for the RHEED specular intensity, τ_{Te}, is nothing but to the period required for the precipitates to vanish. Subsequent impingement of the Te_2 beam, after the annihilation of the precipitates, changes the Pd-terminated $(\sqrt{3}\times\sqrt{3})R30°$ surface back to a Te-terminated (1×1) surface [Fig. 5(f)].

IV. CONCLUSIONS

The impingement of a Pd beam on a Te-terminated PdTe(001)-(1×1) surface transforms the surface structure into Pd-terminated PdTe(001)-$(\sqrt{3}\times\sqrt{3})R30°$ at the saturation coverage of Pd, 1.75 ML. Excess Pd atoms on the surface, if any, form the surface precipitates of Pd-rich Te composition. The precipitates can be annihilated by the subsequent impingement of a Te_2 molecular beam when the substrate temperature is above the melting point of the precipitates, which is found to be substantially lower than the bulk melting point. After the annihilation, the $(\sqrt{3}\times\sqrt{3})R30°$ surface returns to Te-terminated (1×1) with the rapid change of RHEED intensity. Thus the alternate impingement of Pd and Te_2 molecular beams onto the PdTe surface repeats the generation and annihilation of surface precipitates. In this way, the stoichiometric and surface precipitates free film of PdTe compound can grow epitaxially. The self-annihilation of surface precipitates on the compound is a key process to form a stoichiometric intermetallic compound film.

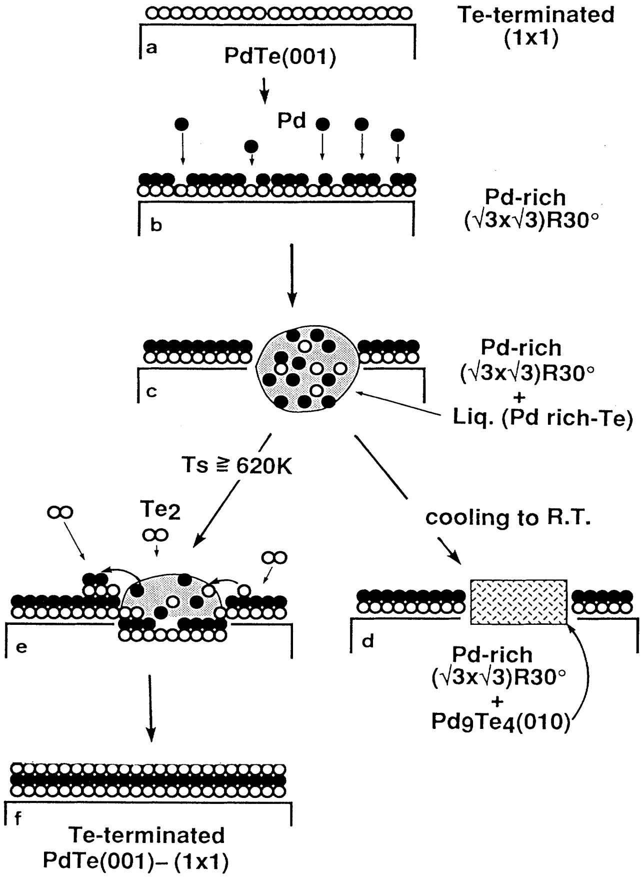

FIG. 5. Mechanism for self-annihilation of surface precipitates in the epitaxial growth of PdTe.

ACKNOWLEDGMENTS

Stimulating discussions with Dr. N. Koguchi, Dr. T. Chikyow, and Dr. T. Hirano are gratefully acknowledged. We are indebted to Dr. S. Takahashi for the HRSEM observation.

[1] N. Miller, J. Vac. Sci. Technol. B **10**, 803 (1992).

[2] K. Takahashi, H. Kawada, S. Ueda, M. Furuse, and S. Shirayone, J. Vac. Sci. Technol. A **9**, 854 (1991).

[3] T. D. Lowes and M. Zinke-Allmang, J. Appl. Phys. **73**, 4937 (1993).

[4] S. Yu Karpov, Yu. V. Kovalchuk, V. E. Myachin, and Yu. V. Pogorelskii, J. Cryst. Growth **129**, 563 (1993).

[5] Y. Horikoshi, M. Kawashima, and H. Yamaguchi, Jpn. J. Appl. Phys. **25**, L868 (1986).

[6] N. Kobayashi, T. Makimoto, and Y. Horikoshi, Jpn. J. Appl. Phys. **24**, L962 (1985).

[7] S. Takahashi and N. Koguchi, *9th Record of Alloy Semiconductor Physics and Electronics Symposium* (Konshou-Electronics, Shizuoka, 1990), p. 117.

[8] N. Koguchi, S. Takahashi, and T. Chikyow, J. Cryst. Growth **111**, 688 (1991).

[9] J. Y. Tsao, J. Cryst. Growth **110**, 595 (1991).

[10] M. Yata, K. Nakamura, and K. Ogawa, J. Vac. Sci. Technol. A **9**, 3019 (1991).

[11] CH. J. Raub, V. B. Compton, T. H. Geballe, B. T. Matthias, J. P. Maita, and G. W. Hull, Jr., J. Phys. Chem. Solids **26**, 2051 (1965).

[12] T. Suntola and M. Antson, U. S. Patent No. 4058430 (1977).

[13] M. Pessa, P. Huttunen, and M. A. Herman, J. Appl. Phys. **54**, 6047 (1983).

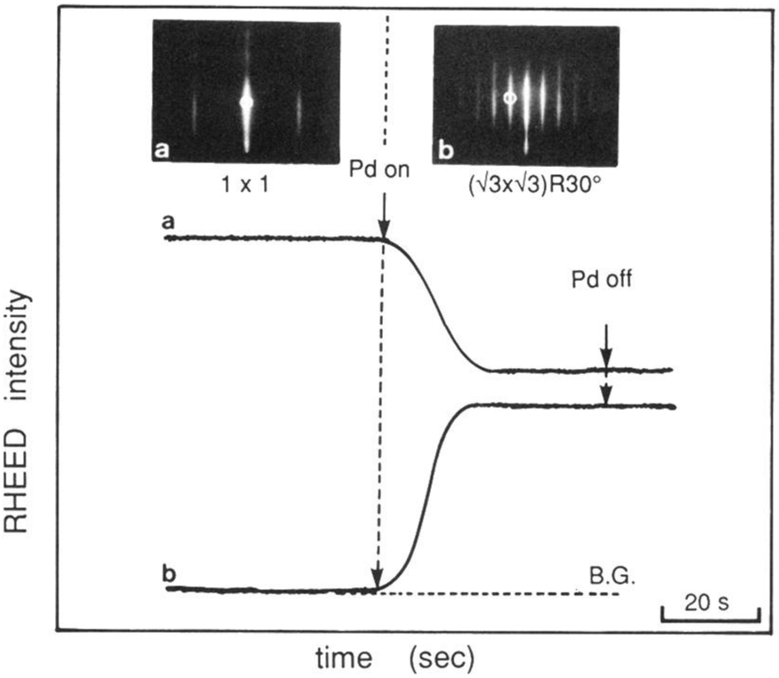

FIG. 1. Changes of the RHEED intensity and the corresponding RHEED patterns during the impingement of the Pd beam on PdTe(001). Curve a: specular intensity. Curve b: intensity of $\frac{1}{3}\,\frac{1}{3}$ fractional order reflection. Pattern (a): surface structure of Te-terminated PdTe(001)-(1×1). The position at which the specular intensity was measured is shown by the white open circle. Pattern (b): surface reconstructed structure of the Pd-terminated or Pd-rich PdTe(001)-$(\sqrt{3}\times\sqrt{3})R\,30°$. The position at which the intensity of $\frac{1}{3}\,\frac{1}{3}$ fractional order reflection was measured is shown by the white open circle.

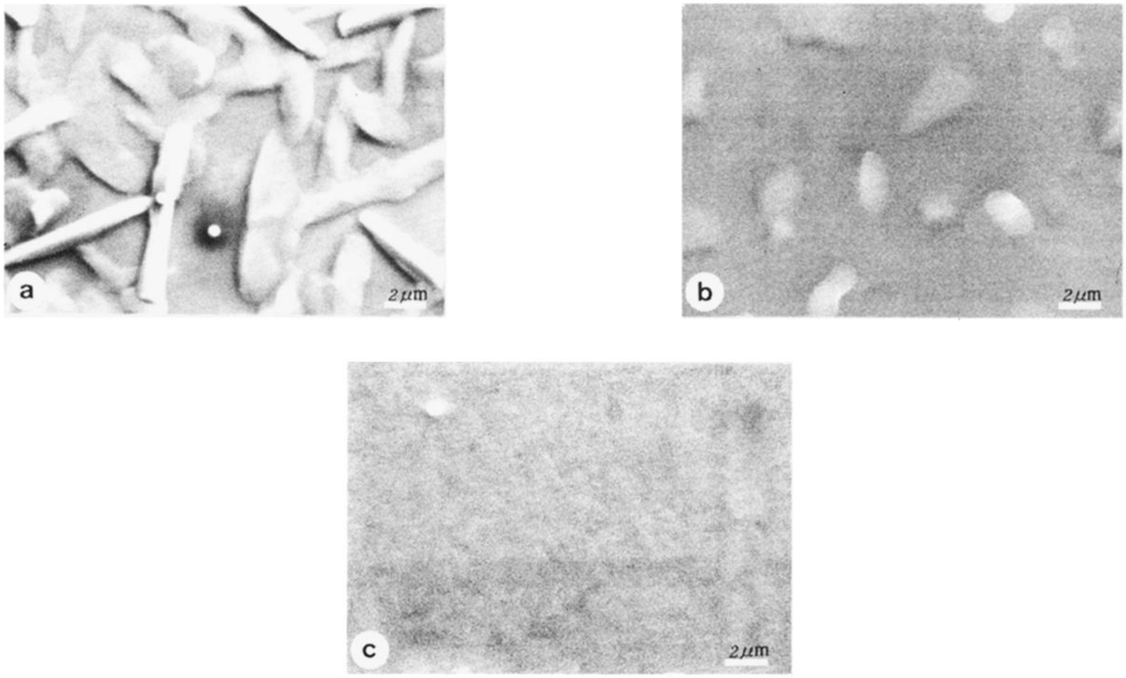

FIG. 2. Surface morphology of the sample. (a) Pd-rich PdTe(001)-($\sqrt{3}\times\sqrt{3}$)$R\,30°$ surface. The precipitates of Pd_9Te_4 (010) existed on the underlying PdTe surface. (b) Pd-rich PdTe(001)-($\sqrt{3}\times\sqrt{3}$)$R\,30°$ surface after the impingement of a Te_2 beam. The exposure time of the Te_2 beam was shorter than τ_{Te}. (c) Te-terminated PdTe(001)-(1×1) surface after the annihilation of the Pd_9Te_4(010) precipitates.

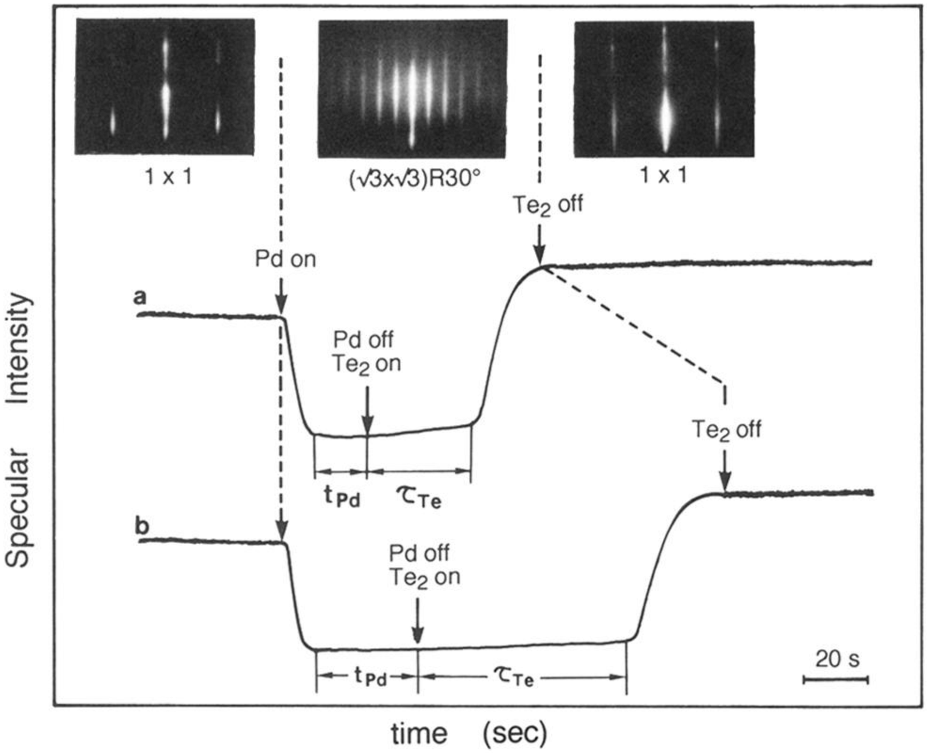

FIG. 3. Changes of the RHEED specular intensity and the corresponding RHEED patterns during alternate impingement of Pd and Te_2 beams. Curve *a*: $t_{Pd}=15$ s; curve *b*: $t_{Pd}=30$ s. $J(Pd)=1.7\times10^{14}$ atoms/cm^2 s. $J(Te_2)=4.0\times10^{13}$ molecules/cm^2 s.